

Characterization of Type II Ligands in CYP2C9 and CYP3A4

Marie M. Ahlström^{*,†,‡} and Ismael Zamora^{§,△}

Discovery DMPK and Bioanalytical Chemistry, AstraZeneca R&D Mölndal, SE-431 83 Mölndal, Sweden, Department of Chemistry, Medicinal Chemistry, Göteborg University, SE-412 96 Gothenburg, Sweden, Lead Molecular Design, S.L., Vallés 96-102 (27) E-08190, Sant Cugat del Vallés, Spain, and Institut Municipal d'Investigació Mèdica (IMIM), Universitat Pompeu Fabra, Doctor Aiguader 80, 08003 Barcelona, Spain

Received September 10, 2007

Type II cytochrome P450 (CYP) ligands cause inhibition by direct coordination to the heme iron atom. This interaction usually leads to high inhibitory potential, which can cause drug–drug interaction. The approach to design compounds with diminished CYP inhibition is different depending on whether the compound binds (type II ligand) or not (type I ligand) to the iron atom of the heme group. In this study, the structural characteristics of nitrogen-containing compounds, which bind to the iron atom in two CYP isoforms (CYP2C9 and CYP3A4), were investigated. The *in vitro* assays applied were fluorescence inhibition assay, difference spectra measurements, and K_s determination. Computational modeling as an alternative method to difference spectra measurements to distinguish between type I and type II ligands was also explored. Since two CYP isoforms were used, information about the isoform specificity of type II ligands was also analyzed. The *in silico* method developed in this study applied together with the information gained from the experimental measurements may result in better decisions during the drug discovery process.

Introduction

The cytochrome P450 (CYP) enzymes^a play an essential role in the metabolism of xenobiotics by catalyzing the monooxygenation of a broad diversity of substrates. CYPs are most abundant in the liver, where a few isoforms, CYP1A2, CYP2C9, CYP2D6, and CYP3A4, account for 80% of the total hepatic metabolism.¹ Inhibition of CYPs can lead to a high risk of drug–drug interactions with potentially serious clinical implications.² Therefore, it is of high importance to discover these inhibitors and to reduce their inhibition potential early in the development of new chemical entities. Some nitrogen-containing heteroaromatic xenobiotics such as pyridine, imidazole, and triazole derivatives³ are known to inhibit CYP enzymes by direct coordination to the heme iron (type II ligands).⁴ The approach to the design of new compounds with a decreased CYP inhibition profile is different depending on the type of inhibition. In the case of a type I ligand, which does not coordinate to the iron atom in the heme group, the design involves disruption of the interactions with amino acids in the active site. For compounds that bind to the heme iron atom, i.e., type II ligands, the strategy is instead to break the nitrogen–iron bond. Therefore, it would be desirable to be able to determine if the CYP inhibition is due to direct coordination to the heme iron atom or not. Modeling of the direct coordination to the heme has been published by Verras et al.; the goal was to find strong azole-based CYP inhibitors.⁵

Experimentally, it is possible to distinguish between type I and type II ligands by UV spectral analysis. The binding of a type II ligand to the pentacoordinated heme iron atom of the

CYP enzyme causes a spin shift of the iron from the high to the low spin state. This shift is characterized by a difference spectrum with a Soret maximum at 425–435 nm and a trough at 390–405 nm. The binding of a type I ligand is characterized by a difference spectrum with a Soret maximum at 385–390 nm and a trough at 420 nm.⁶ The ability of difference spectra to accentuate changes in the high-spin state makes them more apt to reveal multiple substrate binding modes and/or binding modes that are more peripheral to the heme group.⁷ Therefore, difference spectra and not absolute spectra were used in the experimental study for the determination of the binding mode of the compounds.

In this study, the structural characteristics of type II ligands were investigated by measuring CYP inhibition, difference spectra, and the spectral dissociation constant (K_s) for a subset of selected nitrogen-containing compounds. The possibility of distinguishing between type I and type II ligands by modeling direct coordination to the heme was also investigated. Two CYP isoforms were used, CYP2C9 and CYP3A4, which provided information about the isoform specificity of type II ligands.

Results and Discussion

Compound Selection. The selection of the set of compounds to use in the *in vitro* assays that allows the analysis of type II ligands was based on the hypothesis that the binding of ligands is affected by the size of the active site and the steric hindrance,^{8–10} basicity,^{11,12} and lipophilicity^{13,14} of the ligand. In order to study the different factors that may influence the binding of compounds, two different types of interactions were considered, i.e., the part of the ligand that might interact with the heme and the part of the ligand that might interact with amino acids in the active site. Therefore, the goal was to select two different compound classes with (a) identical heme-interacting groups but different active site interacting groups and (b) identical active site interacting groups but different heme-interacting groups (Figure 1). It was not possible to find commercially available compounds with identical interacting groups; instead, the selection of compounds was based on a

* To whom correspondence should be addressed at AstraZeneca R&D Mölndal. Tel: +46 31 776 1274. Fax: +46 31 776 3787. E-mail: marie.m.ahlstrom@astrazeneca.com.

[†] AstraZeneca R&D Mölndal.

[‡] Göteborg University.

[§] Lead Molecular Design, S.L.

[△] Universitat Pompeu Fabra.

^a Abbreviations: ACD, Available Chemicals Directory; CYP, cytochrome P450 enzyme; SHOP, Scaffold HOpping; MFC, 7-methoxy-4-trifluoromethylcoumarin; BFC, 7-benzoyloxy-4-(trifluoromethyl)coumarin.

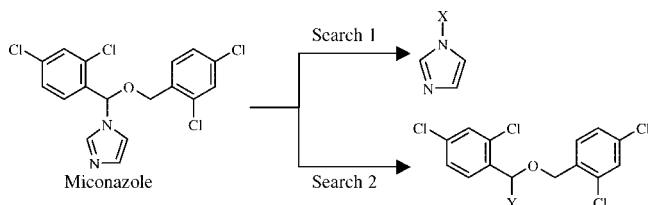


Figure 1. Miconazole was used as a query in the searchable database, created in the program SHOP. One search (search 1) was performed to find compounds with similar heme-interacting groups containing different active site interacting groups (X) and another search (search 2) to find compounds with similar active site interacting groups but with different heme-interacting groups (Y).

similarity search where the interaction pattern of different groups was compared. The starting point was to build a database containing compounds with typical type II ligand groups containing nitrogen atoms with different coordination properties. This was achieved by performing a compound substructure search (Table 1) in the MDL Available Chemicals Directory (MDL ACD) using a size filter of 300–500 Da. The hits from the substructure search in the MDL ACD database were added to the program SHOP,^{15,16} where a searchable database was generated. The default parameters were used to generate the SHOP database. Two searches, using the default parameters, were performed: (search 1) to find compounds with similar heme-interacting groups but different active site interaction patterns and (search 2) to find compounds with similar active site interaction patterns but different heme-interacting groups (Figure 1). The well-characterized type II ligand 1-(2,4-dichlorobenzyl)-[(2,4-dichlorobenzyl)oxy]phenethylimidazole (miconazole) was used as a query.¹⁷

The compounds selected from search 2 can be divided into two classes based on the heme-interacting group: one class based on pyridine (**1**, **2**, **8**–**14**) and one on triazole (**16**–**18**) derivatives (for structures see Table 2). Compound **14**, which has two methyl groups flanking the pyridine nitrogen atom, was selected to investigate the influence of steric hindrance on the interaction with the heme. To investigate if the nitrogen atoms in the central pyrimidine ring **8** could participate in type II binding, a structural analogue without the pyridine was selected (**7**). From search 1, where compounds with similar heme-interacting groups were identified, different nitrogen-containing compounds were selected. The compounds contained moieties such as tetrazole (**3**), isoxazole (**4**), imidazole (**19**), both a triazole and a pyrazole (**20**), and imidazole (**15** and **21**). In the case of pyridines, a series of 2- (**9**), 3- (**10**), and 4-substituted (**11**) pyridines were selected. In addition to the compounds that have the coordinating nitrogen-containing group positioned in one end of the molecule, two compounds with the nitrogen-containing heterocycle in the center of the molecule were selected. These compounds contained an isoxazole (**5**), pyrimidine (**7**), and a triazole moiety (**6**), respectively.

Difference Spectra and Inhibition Measurements. The inhibition of recombinant human CYP2C9 and CYP3A4 was measured as the ability to perform a demethylation of 7-methoxy-4-trifluoromethylcoumarin (MFC) or a debenzoylation of 7-benzyloxy-4-trifluoromethylcoumarin (BFC), respectively. The type of inhibition was examined in detail by determining the spectral binding properties of compounds **1**–**21**. The membrane-bound enzymes usually used in fluorescence inhibition assays could not be used in the difference spectra measurements because of too high turbidity; instead, soluble purified CYP2C9 and CYP3A4 were used. The results provided a comprehensive picture of the inhibition of CYP2C9 and CYP3A4 in the

presence of nitrogen-containing heteroaromatic compounds (Table 2). Compounds containing 4-substituted pyridines (**1**, **2**, **8**, **11**, **12**, and **13**) were classified as type II ligands in both CYP isoforms except compound **2**, which only showed a type II spectrum in CYP3A4. This result was somewhat surprising since **2** is an analogue to **1**, which was classified as a type II ligand in both enzymes. Compound **14**, which contained a 2,6-disubstituted 4-pyridine moiety, showed a characteristic type I spectrum in both CYP isoforms. This means that the water molecule ligated to the heme iron had been displaced, but no direct coordination to the heme iron was achieved. This demonstrated that the compound was bound in the active site but that the pyridine nitrogen atom was sterically hindered and not able to interact with the heme. Compounds with sterically accessible triazoles could be classified as type II ligands. However, if the triazole was located in the center of the molecule (**6**) a characteristic type I spectrum was achieved using CYP2C9, but no clear difference spectrum was achieved using CYP3A4.

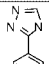
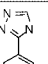
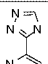
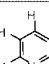
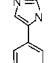
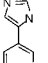
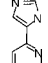
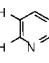
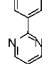
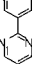
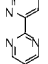
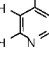
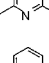
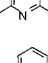
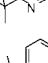

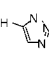
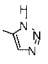
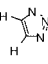

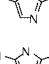
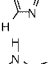
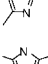

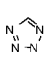
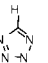
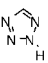

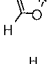
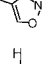
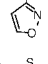

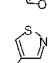
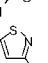
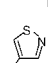



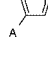

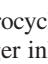
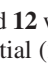


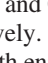
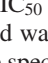

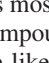

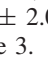

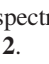
Isoxazoles **4** and **5** did not show type II spectra in any of the two CYP isoforms; hence, this structural moiety does not interact directly with the heme iron. The IC₅₀ values showed that the compounds interacted with the active site and caused moderate inhibition of both enzymes. This active-site interaction was also detected with difference spectra for **4**, which showed a typical type I pattern. Compound **5**, on the other hand, did not show any shift. This observation demonstrated that the accessible isoxazole group in **4** probably displaced the ligated water molecule. Compound **5** could not remove the ligated water molecule; the isoxazole moiety is not as accessible in **5** as in **4**. Therefore, the inhibition of CYP2C9 (IC₅₀ = 39 μM) and CYP3A4 (IC₅₀ = 33 μM) should be due to interactions with the active site further away from the ligated water molecule.

The imidazoles (**15**, **19**, **20**, and **21**) showed inhibition of both CYP isoforms; the IC₅₀ value was 10-fold lower for CYP3A4 compared to CYP2C9. Type II spectra were recorded for these compounds, which indicated that the strong inhibition was due to direct coordination of the imidazole ring to the heme iron. Introducing two additional nitrogen atoms in the heterocyclic ring (tetrazole) reduces the coordination potential via the nitrogen electron pair due to the electron-withdrawing effect of the additional nitrogen atoms.¹⁸ Tetrazoles have been reported to be substrates¹⁹ and weak inhibitors²⁰ of CYP2C9, but the type of interaction has not been established. The tetrazole (**3**) did not show strong inhibition of CYP2C9 or CYP3A4; UV absorbance of the ligand unfortunately prevented further characterization of the binding spectra.

The series of compounds with 2- (**9**), 3- (**10**), or 4-substituted (**11**) pyridine moieties demonstrates how the inhibitory potential increased when the nitrogen atom was moved from the 2- to the 4-position (Table 2). This trend was observed in both CYP3A4 and CYP2C9. Additional measurements of the binding of these compounds in CYP3A4 showed that they interacted with the active site in different modes. No difference spectra could be detected for **9**; hence, the minor inhibition caused by **9** was not due to direct coordination to the heme iron. Compounds **10** and **11** were type II ligands, but the 4-substituted pyridine derivative (**11**) had a lower spectral binding constant for CYP3A4 (data not shown) compared to the 3-substituted derivative (**10**).

One explanation to why nitrogen-containing compounds showed larger inhibition potential in CYP3A4 compared to CYP2C9 could be the larger active site of CYP3A4 (Figure 2a), compared to CYP2C9 (Figure 2b). In the CYP3A4 cavity, the heme iron atom is more accessible for direct interaction with

Table 1. Substructures Used in the MDL ACD Search and the Number of Hits Identified

Sub-structure	Hits	Sub-structure	Hits	Sub-structure	Hits	Sub-structure	Hits
	526		330		224		2173
	11		0		0		1992
	354		392		224		2888
	34		0		0		0
	32		0		0		14
	115		2		2		171
	325		13		0		0
	318		0		0		9929
	1236		80		12		72
	15		265		41		0
	6		0		0		0
	0		0		6		0
	0		87		321		0

the nitrogen-containing heterocycles. Compound **12** was the only compound that had a stronger inhibition potential (20-fold) for CYP2C9 than for CYP3A4. The structural analogue **13** showed equal inhibition of CYP2C9 and CYP3A4; the IC_{50} values were 0.50 and 0.23 μM , respectively. The compound was characterized as a type II ligand in both enzymes, but the spectral binding constant was almost 10-fold lower for CYP3A4 ($K_s = 0.38 \pm 0.086 \mu M$) compared to CYP2C9 ($K_s = 3.6 \pm 2.0 \mu M$). The titrated difference spectra are shown in Figure 3.

Compound **8** showed a strong inhibition ($IC_{50} = 1.3 \mu M$) of CYP3A4, and spectral studies showed that the inhibition was due to direct coordination to the heme iron. The structural analogue **7**, which lacks the pyridine moiety, did not inhibit CYP3A4 and did not show a type II spectrum. These data illustrate that the nitrogen atoms in the central pyrimidine ring could not interact directly with the heme iron due to the surrounding bulky groups. Compound **17** had a 30-fold lower IC_{50} value in CYP3A4 than its structural analogue **18**. The difference spectrum showed that the main contribution to the inhibition was due to direct coordination to the heme iron. Further studies of these interactions, including K_s measurements, showed that **17** ($K_s = 0.21 \pm 0.076 \mu M$) had a 16-fold lower spectral binding constant for CYP3A4 (Figure 4a) than compound **18** ($K_s = 3.5 \pm 1.9 \mu M$) (Figure 4b). The heme-interacting groups are the same in these two compounds; hence, the lower spectral binding constant in **17** seems to be due to

more favorable interactions in the binding pocket compared to that of **18**. Compounds with a high IC_{50} value ($>50 \mu M$) could be type II ligands (**8** and **20**), but within this subset of compounds most of the type II ligands had an IC_{50} value below 20 μM . Compounds **1** and **2** illustrated, in the same way as **17** and **18**, the likely influence of the amino acid interactions for type II ligands. The two compounds showed typical type II difference spectra with CYP3A4, but **1** had a 30-fold lower IC_{50} value than **2**.

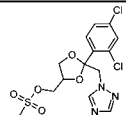
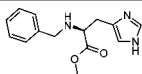
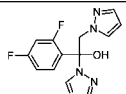
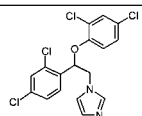
Computational Modeling. Compounds that inhibit one or several CYP isoforms may cause drug–drug interactions. The modifications to alter the inhibition are different depending on the type of binding. For this reason, it would be helpful to be able to predict if a compound is a type I or a type II ligand. Difference spectra from a type II ligand are correlated with the presence of a nitrogen atom with an electron pair sterically accessible.²³ Therefore, one way to discriminate between type I and type II ligands would be to investigate if the compounds contain any sterically accessible nitrogen atom that can coordinate to the heme iron atom. Another important characteristic to take into account during the modeling is the direction of interaction, i.e., the direction of the orbital containing the lone pair of the nitrogen atom.

To be able to study this a grid probe, mimicking the heme, was generated. This probe does not contain the heme carboxylic acid chains because they do not contribute to the

Table 2. Binding Type, IC₅₀ Values, and Calculated ClogP of 1–21 in CYP2C9 and CYP3A4

Cmpd	Structure	CLogP	IC ₅₀ (μM)		Binding Type min (nm)/max (nm)	
			CYP2C9	CYP3A4	CYP2C9	CYP3A4
1		4.97	4.3 ± 0.4	1.3 ± 0.2	Type II 411/431	Type II 408/428
2		3.32	>50	28 ± 2.4	N.D ^a	Type II 411/430
3		1.72	>30	34 ± 2.4	N.D ^b	N.D ^b
4		3.98	11 ± 0.8	12 ± 0.9	Type I 419/381	Type I 414/377
5		3.82	39 ± 2.5	33 ± 1.9	N.D ^a	N.D ^a
6		3.65	N.D ^c	>20	Type I 422/378	N.D ^a
7		3.58	>50	>40	N.D ^a	N.D ^a
8		2.62	>50	1.3 ± 0.2	Type II 412/430	Type II 410/428
9		3.79	>50	>40	N.D ^a	N.D ^a
10		3.53	21 ± 1.8	9.6 ± 1.2	Type II 411/428	Type II 409/423
11		3.47	4.8 ± 0.5	0.071 ± 0.01	Type II 412/431	Type II 410/427
12		2.94	1.3 ± 0.2	26 ± 2.6	Type II 411/429	Type II 410/429
13		4.98	0.5 ± 0.08	0.23 ± 0.08	Type II 411/431 K _s = 3.6 μM	Type II 407/428 K _s = 0.38 μM
14		4.35	>50	13 ± 1.3	Type I 418/382	Type I 416/384
15		4.26	0.22 ± 0.04	0.045 ± 0.007	Type II 413/435	Type II 409/431
16		3.91	8.1 ± 0.6	0.13 ± 0.03	Type II 410/430	Type II 407/428
17		2.91	>50	0.21 ± 0.04	Type II 410/430	Type II 406/427 K _s = 0.21 μM

Table 2. Continued

Cmpd	Structure	CLogP	IC ₅₀ (μM)		Binding Type min (nm)/max (nm)	
			CYP2C9	CYP3A4	CYP2C9	CYP3A4
18		2.72	>50	7.7 ± 0.9	Type II 411/428	Type II 406/428 K _s = 3.5 μM
19		2.20	20 ± 2.7	1.5 ± 0.08	Type II 412/433	Type II 409/431
20		0.89	>50	44 ± 4.2	Type II 408/427	Type II 399/427
21		5.75	10 ± 0.6	0.06 ± 0.008	Type II 412/432	Type II 412/430

^a No shift. ^b Ligand absorbance prevented characterization. ^c Ligand fluorescence prevented IC₅₀ determination.

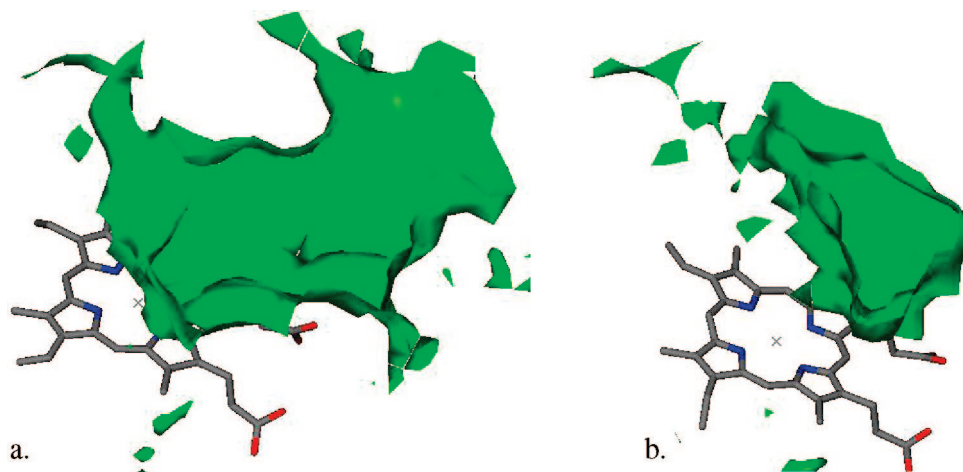


Figure 2. Analysis of the active site cavities of (a) CYP3A4 (PDB: 2J0C)²¹ and (b) CYP2C9 (PDB: 1R9O)²² using GRID fields, which illustrates the larger active site of CYP3A4 compared to CYP2C9. The analysis was done in the flexible mode, using the C3 probe at -0.1 kcal/mol, with a grid step of 0.5 Å covering only the heme proximity.

interaction between the iron and the nitrogen atom of the ligand. The compound structures were submitted as smiles strings and converted to mol2 files using Mizer.²⁴ The approach to generate conformations was to dock the compounds in the active site of CYP3A4 (PDB: 2J0C) using the GRID^{25,26}-based program GLUE.²⁴ The docking conformations within 5 Å from the heme were used for the study, and approximately four conformers of each compound were within this distance. The isoform CYP3A4 was used because of its large less restrictive active site. This approach to generate conformers will add information from the active site into the conformers. Finding potential interacting nitrogen atoms was achieved by MoKa,²⁴ which was used for the pK_a calculations. To guarantee that at least 50% of the compounds would be uncharged at pH 7.4, only the nitrogen atoms with a pK_a lower than 6.5 were taken into account for further computation. The orientation of the orbital containing the lone pair was taken into account by the addition of a reference point 1.5 Å from the basic nitrogen. When calculating the direction of this reference point, the three atoms bound to the nitrogen atom were used for sp³-hybridized nitrogen atoms (Figure 5a), while for sp²-hybridized nitrogen atoms

the two atoms bound to the nitrogen atom plus the atom in the 4-position to the nitrogen atom were used (Figure 5b).

A grid box is defined around the molecule, and the grid points used in the calculation were within a radius of 5 Å from the reference point. To decrease the amount of time needed for the calculation, all grid points within a radius of 2 Å from the nitrogen atom were deleted (Figure 6a). This could be done without affecting the quality of the modeling because no interactions can take place that close to the nitrogen. The orientation of the probe was optimized at each grid point to minimize the angle between the line formed between the nitrogen atom and the lone pair and the line between the iron atom and the nitrogen atom (Figure 6b). When the heme was positioned according to these geometrical parameters, the interaction energy between the basic nitrogen atom in the ligand and the atoms in the heme probe were calculated. The total interaction energy (E_{tot}) is the sum of interactions (E_i) multiplied by a penalty function (eq 1).

$$E_{\text{tot}} = \sum_{\text{atom}} E_i e^{-\frac{(a-0)^2}{20}} \quad (1)$$

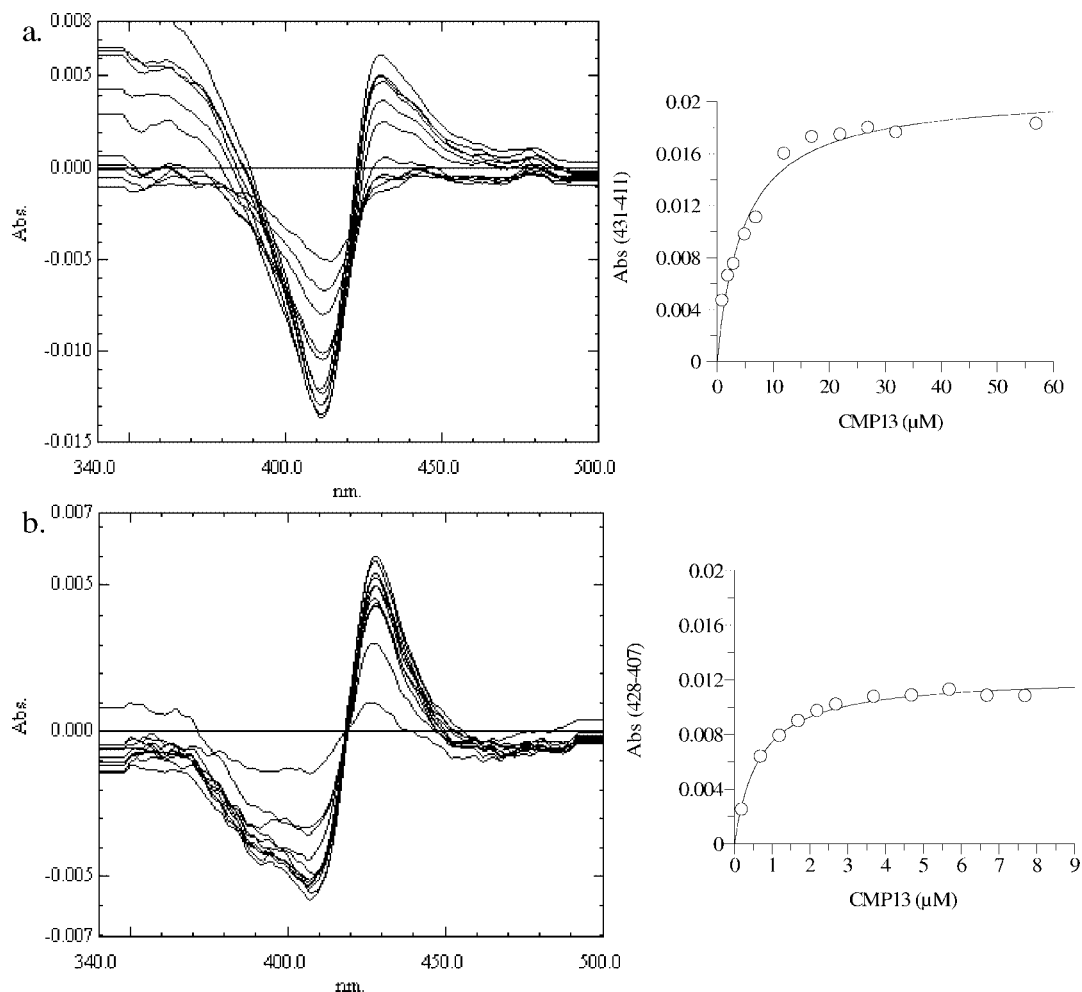


Figure 3. Binding spectra of compound **13** in 50 mM potassium phosphate buffer, pH 7.4 containing 200 mM KCl, 2 mM DTT, 1 mM EDTA, and 20% glycerol (v/v) in 1 μ M CYP2C9 (a) or CYP3A4 (b).

The two angles (90° and 180°) shown in Figure 6c are the average values calculated from crystal structures available in PDB. The criterion was that the heme protein should be cocrystallized with a ligand that contains a nitrogen atom, which coordinates to the heme moiety. Observations from these crystal structures indicated that the heme plane should be kept perpendicular to the line formed by the nitrogen and the iron atoms. If the angle deviates more than 20° from the optimal angle (180°) between the sulfur, iron, and the nitrogen atom, the penalty function will decrease the total interaction energy (E_{tot}).

Compounds **4** and **14**, which show distinct type I difference spectra in both CYP isoforms, were correctly predicted as type I ligands. The compounds that showed evident type II difference spectra (**1**, **8**, **10–13**, and **15–21**) in both CYP isoforms were correctly predicted as type II ligands. No difference spectra in any of the CYP isoforms could be detected for **3**, **5**, **7**, and **9**. This phenomenon has previously been reported for known type I ligands such as diclofenac, (*S*)-warfarin, flurbiprofen, naproxen, and phenytoin.^{27–29} Since no difference spectra were obtained, it could not be determined if the compounds were type I or type II ligands, and therefore, it was not possible to evaluate the predictions of these compounds. The compounds tested in this study indicate that a difference spectrum is achieved if the compound is a strong type II ligand. This is due to the fact that direct coordination to the heme iron is strong and the majority of the enzyme molecules will

exist in the low spin state. It is more difficult to achieve a type I than a type II spectrum because of the absence of strong interaction with the heme iron atom. Instead, several binding modes within the active site of the enzyme are possible, where in some cases the compound displaces the ligated water molecule and in some cases not. Hence, the mixture of enzyme and ligand could contain some enzyme molecules in the high spin state and some in the low spin state, which means that no difference spectra can be achieved. Considering this, the compounds with no difference spectra (**3**, **5**, **7**, and **9**) were assumed to be type I ligands. If this assumption is valid the predictions of **3** and **7** were correct, as these compounds were predicted to be type I ligands. Compounds **5** and **9** on the other hand were predicted to be type II ligands, which then should be “incorrect”. These initial predictions were only based on the interactions of the compounds with the heme probe, which means that the model was isoform independent. To perform a complete prediction, the analysis should include structural information about the specific isoform. That can be accomplished by the alignment of the compound and the heme probe with the isoform of interest using the heme in the crystal structure as a reference. After this step the atom that interacts with the heme iron is fixed only allowing the other part of the compound to move inside the active site. This showed that compounds **5** and **9** could not fit into the active site when the nitrogen atom was coordinated to the heme iron, they were too sterically hindered around the nitrogen atom.

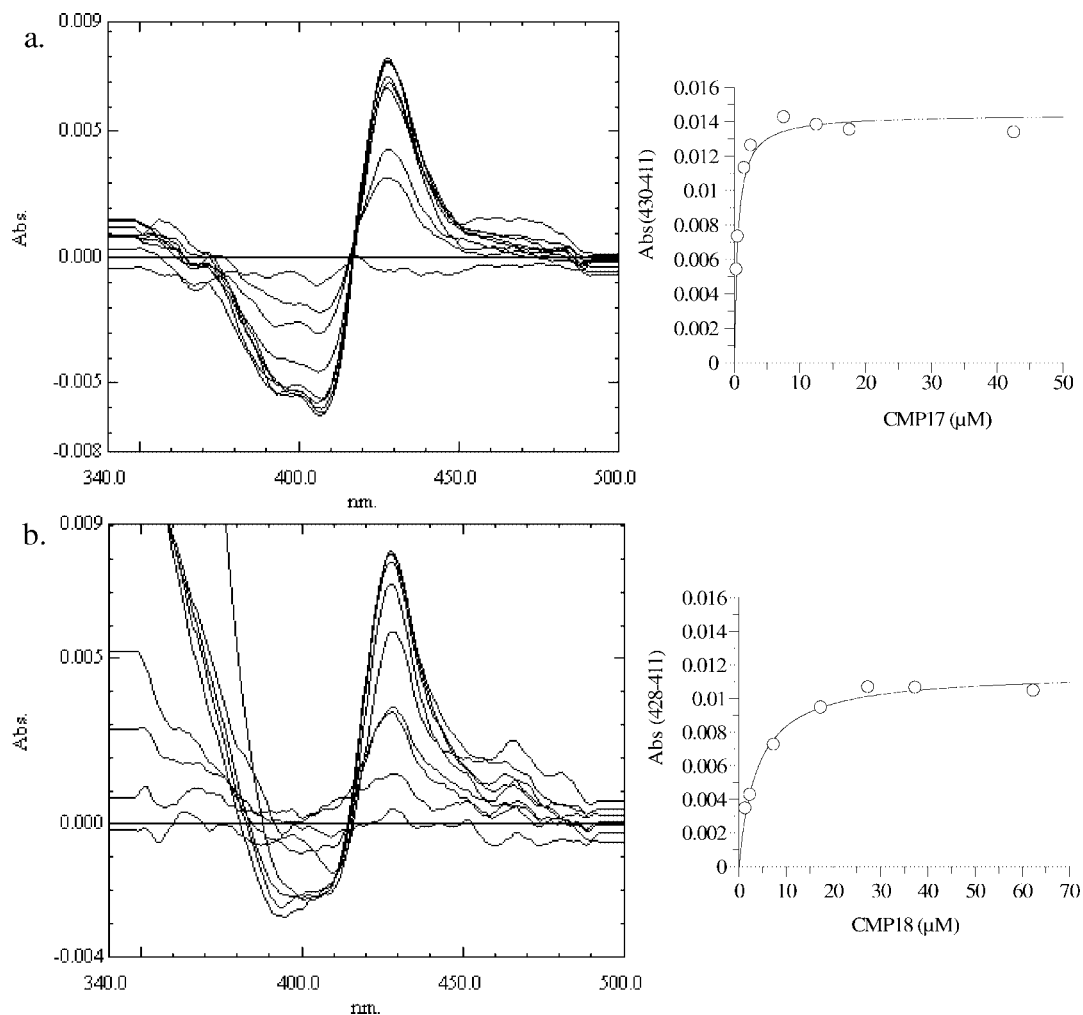


Figure 4. Binding spectra of 1 μM CYP3A4 in 50 mM potassium phosphate buffer, pH 7.4 containing 200 mM KCl, 2 mM DTT, 1 mM EDTA, and 20% glycerol (v/v) and compound **17** (a) or compound **18** (b).

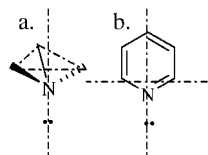


Figure 5. Calculation of the orientation of the orbital containing the lone pair. (a) In the case of an aliphatic nitrogen, the three atoms bound to the nitrogen atom were used. (b) In the case of an aromatic nitrogen atom, the two neighboring and 4-positioned atoms were used for the calculation.

Hence, this shows that the compounds could not be classified as type II ligands.

Conclusions

The binding of a ligand to the heme in cytochrome P450 enzymes is influenced not only by the coordination of substrates to the heme iron but also by the interactions between the compound and the active site amino acids. To be able to discriminate between type I and type II ligands one important factor to consider is the orientation of the orbital that contains the lone pair of the nitrogen atom. The driving force in docking procedures is mainly electrostatic, which is independent of this factor. The script developed in this study considers the direction of the orbital. Using this information together with information about the active site structure of the specific CYP isoform active

site provided a model, which could discriminate between type I and type II ligands. The set of compounds tested has considerably increased the knowledge about interactions important for binding of type II ligands in CYP3A4 and CYP2C9. All 4-pyridines were type II inhibitors, and this inhibition potential was decreased when the nitrogen atom was moved from the 4-position to the 2-position. Isoxazole and tetrazole moieties did not interact with the heme iron atom, while the compounds that contained sterically accessible triazoles, were classified as type II inhibitors. Compounds interacting with the heme iron atom do not necessarily have strong inhibitory potential (**8**, **17**, **18**, and **19**) and a type II ligand can show strong inhibitory potential for one isoform, but not for another (**17**). The method developed in this study can be a valuable tool in the drug discovery process when designing compounds with decreased or no inhibition potential. This together with the information gained from the experimental measurements may result in better decisions during the drug discovery process.

Experimental Section

Materials. Sulfaphenazole, ketoconazole, 7-methoxy-4-trifluoromethylcoumarin (MFC), KCl, DTT (D,L-dithiothreitol), EDTA (ethylenediaminetetraacetic acid trisodium salt), and NADPH were purchased from Sigma Chemical Co. (St. Louis, MO, USA). 7-Benzyloxy-4-(trifluoromethyl)coumarin (BFC) was purchased from BD Bioscience (Erembodegem, Belgium). K_2HPO_4 and

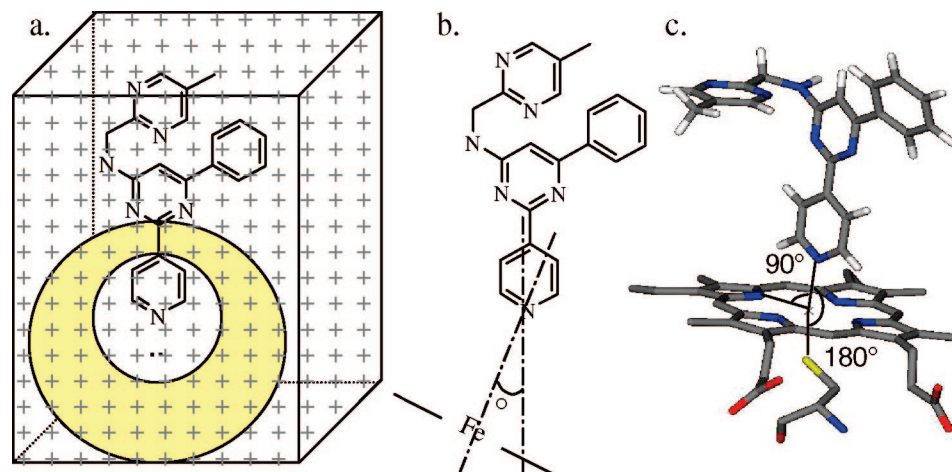


Figure 6. (a) Grid points used in the script are within the yellow area. (b) Optimization of the angle between the lines formed between the nitrogen atom and the lone pair and the line between the iron and the nitrogen atom. (c) Empirical mean values of the angles calculated from all available heme proteins cocrystallized with ligands that contain a basic nitrogen atom, which coordinate to the heme moiety.

Table 3. Fluorescence Assay Conditions

in vitro assay	enzyme (pmol)	KPO ₄ buffer pH 7.4 (mM)	substrate (μM)	NADPH (mM)	incubation time (min)
CYP2C9	3.0	0.025	50	1	50
CYP3A4	2.0	0.20	13	1	50

KH₂PO₄ were purchased from Kebo Laboratory (Stockholm, Sweden) and acetonitrile and formic acid from Merck (Darmstadt, Germany).

Enzymes. Recombinant human CYP2C9 and CYP3A4 expressed in *Saccharomyces cerevisiae*³⁰ used in the fluorescent inhibition assay and soluble CYP2C9 and CYP3A4 expressed in *E. coli*²¹ used in the difference spectra analysis were obtained from Astra-Zeneca Biotech Laboratory (Södertälje, Sweden).

Computational Modeling. All calculations were performed in a Linux environment on a 32 MB personal computer. The software utilized in the computational modeling was GRID v. 22, GLUE, Mizer, MoKa, and SHOP v. 2.0 (Molecular Discovery Ltd.). The compounds (**1–21**) were docked into (PDB: 2J0C)²¹ using the GRID^{25,26}-based docking program GLUE.²⁴ The modifications done to the protein were to delete the water molecules and to remove the ligand from the binding site. The PDB file had to be modified before being imported into GLUE, which is performed by Greater that converts the PDB format to the format of the input files (kout files) required to run the docking procedure. The box size used was 20 × 20 × 20 Å, centered round the crystallographic ligand coordinates. The default probes, representing the different atoms,³¹ were used when performing the binding site precalculations in GLUE, and default values were used when performing the docking.

Inhibition Studies. The fluorometric assays³² were done in black Costar 96-well plates (Corning Incorporated, Corning, NY). Addition of reagents to the 96-well plates was done by a multipipette. The total reaction volume was 200 μL, and each reaction mixture contained CYP expressed in *S. cerevisiae*. The enzyme, potassium phosphate (KPO₄) buffer, NADPH, and substrate assay concentrations in the two CYP isoforms are shown in Table 3.

The substrates were dissolved in 40% acetonitrile in water, and the concentrations in the assays were at *K_m*. Test compounds and positive control inhibitors were dissolved in 50% acetonitrile in water. The final acetonitrile concentration in the assay was 2%. Before running the assay, it was verified that the compounds did not interfere with the assay, i.e., fluorescence at the same wavelength as the MFC metabolite (CYP2C9) or BFC metabolite (CYP3A4). The inhibitors were serially diluted to give final concentrations, ranging from 0.018 to 40 μM. Sulfaphenazole was used as a positive control in the CYP2C9 assay and was serially diluted to give final

concentrations, ranging from 0.005 to 12 μM. Ketoconazole was used as a positive control in the CYP3A4 assay and was serially diluted to give final concentrations ranging from 0.001 to 2.0 μM. The reactions were started by the addition of NADPH after a preincubation of 10 min at 37 °C. To stop the reaction, 75 μL of 20% 0.5 M Tris and 80% acetonitrile were added. The fluorescence was measured using a SpectraMax Gemini XS (Molecular Devices Corporation, Sunnyvale, CA).

Difference Spectra. Binding spectra were recorded at room temperature on a Shimadzu UV-2401 PC (Shimadzu Duisburg, Germany), and data were analyzed using UVProbe software (Shimadzu Duisburg, Germany). All experiments were carried out at room temperature in matched microcuvettes (2 mm × 10 mm internal) containing 1 μM purified CYP2C9 or CYP3A4 and 200 mM KCl, 2 mM DTT, 1 mM EDTA, and 20% glycerol (v/v) in 50 mM potassium phosphate buffer pH 7.4. To obtain difference spectra, a baseline was recorded with the CYP enzyme and buffer in both the sample and the reference cuvettes followed by substrate titration into the sample cuvette and solvent titration of the same volume into the reference cuvette. Spectra were recorded between 340 and 500 nm after each substrate aliquot addition. For type I binding, the peak absorbance was ~390 nm and the trough was ~420 nm, while for type II spectra, the trough was ~405 nm and the peak was ~435 nm. To obtain absolute spectra, a baseline was recorded with the buffer mixture in the sample and reference cuvettes. Next, the enzyme was added to the sample cuvette followed by titration of the compound into both cuvettes so that the majority of any interfering signal of the compound was subtracted.

Data Analysis. Nonlinear regression (GraFit version 4.0.13, Erithacus Software Limited, Middlesex, U.K.) was used to determine the IC₅₀ by using the equation $y = \text{range}/(1 + (x/\text{IC}_{50})^s)$. In this equation, range is the fitted uninhibited value, and *s* is a slope factor. The equation assumes that *y* falls with increasing *x*. Because of the high affinities of the ligands (*K_s* within 5-fold of the CYP concentration), a nonlinear regression analysis using a quadratic equation (GraphPad Prism version 4.00, San Diego, CA) was applied to determine the *K_s* for all the ligands reported in this study: $\Delta A = A_0 + (B_{\text{max}}/2[E])\{(K_s + [E] + [L]) - \{(K_s + [E] + [L])^2 - 4[E][L]\}^{1/2}}\}$, where *A* is the absorbance difference, *B_{max}* is the maximum absorbance difference extrapolated to infinite ligand concentration, *L* is the ligand concentration, and *E* is the total enzyme concentration (*A₀* is a coefficient in each analysis and not relevant here).

Acknowledgment. We thank Gisela Brändén for providing us with the purified soluble CYP3A4. We also thank Kristina

Luthman and Marianne Ridderström for helpful discussions and critical reading of the manuscript.

References

- (1) Ortiz de Montellano, P. R. *Cytochrome P450: Structure, Mechanism, and Biochemistry*, 3rd ed.; Plenum: New York, 2005; p 689.
- (2) Fleishaker, J. C.; Herman, B. D.; Carel, B. J.; Azie, N. E. Interaction between ketoconazole and almotriptan in healthy volunteers. *J. Clin. Pharmacol.* **2003**, *43* (4), 423–427.
- (3) Testa, B.; Jenner, P. Inhibitors of Cytochrome P-450s and their mechanism of action. *Drug Metab. Rev.* **1981**, *12* (1), 1–117.
- (4) Ballard, S. A.; Lodola, A.; Tarbit, M. H. A comparative study of 1-substituted imidazole and 1,2,4-triazole antifungal compounds as inhibitors of testosterone hydroxylations catalysed by mouse hepatic microsomal cytochromes P-450. *Biochem. Pharmacol.* **1988**, *37* (24), 4643–51.
- (5) Verras, A.; Kuntz, I. D.; Ortiz de Montellano, P. R. Computer-Assisted Design of Selective Imidazole Inhibitors for Cytochrome P450 Enzymes. *J. Med. Chem.* **2004**, *47*, 3572–3579.
- (6) Schenkman, J. B.; Remmer, H.; Estabrook, R. W. Spectral studies of drug interaction with hepatic microsomal cytochrome. *Mol. Pharmacol.* **1967**, *3* (2), 113–23.
- (7) Locuson, C. W.; Hutzler, J. M.; Tracy, T. S. Visible spectra of type II cytochrome P450-drug complexes: evidence that “incomplete” heme coordination is common. *Drug Metab. Dispos.* **2007**, *35* (4), 614–22.
- (8) Murray, M.; Wilkinson, C. F. Interactions of nitrogen heterocycles with cytochrome P-450 and monooxygenase activity. *Chem.–Biol. Interact.* **1984**, *50* (3), 267–75.
- (9) Rogerson, T. D.; Wilkinson, C. F.; Hetarski, K. Steric factors in the inhibitory interaction of imidazoles with microsomal enzymes. *Biochem. Pharmacol.* **1977**, *26* (11), 1039–42.
- (10) Vaz, A. D.; Coon, M. J.; Peegel, H.; Menon, K. M. Substituted pyridines: nonsteroidal inhibitors of human placental aromatase cytochrome P-450. *Drug Metab. Dispos.* **1992**, *20* (1), 108–12.
- (11) Petzold, D. R.; Rein, H.; Schwarz, D.; Sommer, M.; Ruckpaul, K. Relation between the structure of benzphetamine analogues and their binding properties to cytochrome P-450 LM2. *Biochim. Biophys. Acta* **1985**, *829* (2), 253–61.
- (12) Uptagrove, A. L.; Nelson, W. L. Importance of amine pKa and distribution coefficient in the metabolism of fluorinated propranolol derivatives. Preparation, identification of metabolite regioisomers, and metabolism by CYP2D6. *Drug Metab. Dispos.* **2001**, *29* (11), 1377–88.
- (13) Lewis, D. F.; Lake, B. G.; Dickins, M. Quantitative structure–activity relationships (QSARs) in inhibitors of various cytochromes P450: the importance of compound lipophilicity. *J. Enzyme Inhib. Med. Chem.* **2007**, *22* (1), 1–6.
- (14) Riley, R. J.; Parker, A. J.; Trigg, S.; Manners, C. N. Development of a generalized quantitative physicochemical model of CYP3A4 inhibition for use in early drug discovery. *Pharm. Res.* **2001**, *18* (5), 652–5.
- (15) Ahlstrom, M. M.; Ridderstrom, M.; Luthman, K.; Zamora, I. Virtual screening and scaffold hopping based on GRID molecular interaction fields. *J. Chem. Inf. Modeling* **2005**, *45* (5), 1313–23.
- (16) Bergmann, R.; Linusson, A.; Zamora, I. SHOP: Scaffold HOPping by GRID-Based Similarity Searches. *J. Med. Chem.* **2007**, *50* (11), 2708–2717.
- (17) Rodrigues, A. D.; Gibson, G. G.; Ioannides, C.; Parke, D. V. Interactions of imidazole antifungal agents with purified cytochrome P-450 proteins. *Biochem. Pharmacol.* **1987**, *36* (24), 4277–81.
- (18) Vinh, T. K.; Ahmadi, M.; Delgado, P. O.; Perez, S. F.; Walters, H. M.; Smith, H. J.; Nicholls, P. J.; Simons, C. 1-[(Benzofuran-2-yl)phenylmethyl]-triazoles and -tetrazoles - potent competitive inhibitors of aromatase. *Bioorg. Med. Chem. Lett.* **1999**, *9* (14), 2105–8.
- (19) Mancy, A.; Broto, P.; Dijkstra, S.; Dansette, P. M.; Mansuy, D. The substrate binding site of human liver cytochrome P450 2C9: an approach using designed tienilic acid derivatives and molecular modeling. *Biochemistry* **1995**, *34* (33), 10365–75.
- (20) Taavitsainen, P.; Kiukaanniemi, K.; Pelkonen, O. In vitro inhibition screening of human hepatic P450 enzymes by five angiotensin-II receptor antagonists. *Eur. J. Clin. Pharmacol.* **2000**, *56* (2), 135–40.
- (21) Ekroos, M.; Sjogren, T. Structural basis for ligand promiscuity in cytochrome P450 3A4. *Proc. Natl. Acad. Sci. U.S.A.* **2006**, *103* (37), 13682–7 (see comment).
- (22) Wester, M. R.; Yano, J. K.; Schoch, G. A.; Yang, C.; Griffin, K. J.; Stout, C. D.; Johnson, E. F. The structure of human cytochrome P450 2C9 complexed with flurbiprofen at 2.0-Å resolution. *J. Biol. Chem.* **2004**, *279* (34), 35630–7.
- (23) Mailman, R. B.; Kulkarni, A. P.; Baker, R. C.; Hodgson, E. Cytochrome P-450 difference spectra: effect of chemical structure on type II spectra in mouse hepatic microsomes. *Drug Metab. Dispos.* **1974**, *2* (3), 301–8.
- (24) www.moldiscovery.com. Molecular Discovery Ltd., 215 Marsh Rd, HA5 5NE Pinner, Middlesex, U.K.
- (25) Boobbyer, D. N.; Goodford, P. J.; McWhinnie, P. M.; Wade, R. C. New hydrogen-bond potentials for use in determining energetically favorable binding sites on molecules of known structure. *J. Med. Chem.* **1989**, *32* (5), 1083–94.
- (26) Goodford, P. J. A computational procedure for determining energetically favorable binding sites on biologically important macromolecules. *J. Med. Chem.* **1985**, *28* (7), 849–57.
- (27) Dickmann, L. J.; Locuson, C. W.; Jones, J. P.; Rettie, A. E. Differential roles of Arg97, Asp293, and Arg108 in enzyme stability and substrate specificity of CYP2C9. *Mol. Pharmacol.* **2004**, *65* (4), 842–50.
- (28) Davies, C.; Witham, K.; Scott, J. R.; Pearson, A.; DeVoss, J. J.; Graham, S. E.; Gillam, E. M. Assessment of arginine 97 and lysine 72 as determinants of substrate specificity in cytochrome P450 2C9 (CYP2C9). *Drug Metab. Dispos.* **2004**, *32* (4), 431–6.
- (29) Hummel, M. A.; Locuson, C. W.; Gannett, P. M.; Rock, D. A.; Mosher, C. M.; Rettie, A. E.; Tracy, T. S. CYP2C9 genotype-dependent effects on in vitro drug-drug interactions: switching of benzbromarone effect from inhibition to activation in the CYP2C9.3 variant. *Mol. Pharmacol.* **2005**, *68*, 644–51.
- (30) Masimirembwa, C. M.; Otter, C.; Berg, M.; Jonsson, M.; Leidvik, B.; Jonsson, E.; Johansson, T.; Backman, A.; Edlund, A.; Andersson, T. B. Heterologous expression and kinetic characterization of human cytochromes P-450: validation of a pharmaceutical tool for drug metabolism research. *Drug Metab. Dispos.* **1999**, *27* (10), 1117–22.
- (31) Goodford, P. Multivariate characterization of molecules for QSAR analysis. *J. Chemom.* **1996**, *10*, 107–117.
- (32) Crespi, C. L.; Miller, V. P.; Penman, B. W. Microtiter plate assays for inhibition of human drug-metabolizing cytochromes P450. *Anal. Biochem.* **1997**, *248* (1), 188–90.

JM701121Y